PHYSICAL REVIEW B **66**, 020303(R) (2002)

Patterning and ordering in driven alloys with coupled conserved and nonconserved order parameters

Ji-wen Liu and Pascal Bellon
Department of Materials Science and Engineering and Frederick Seitz Materials Research Laboratory, University of Illinois at Urbana-Champaign, Urbana, Illinois 61801
(Received 24 May 2002; published 24 July 2002)

We study an alloy system with coupled conserved and nonconserved order parameters driven by ballistic jumps with finite range. The dynamical stabilization of nonequilibrium steady states is investigated by using a mean-field kinetic model and kinetic Monte Carlo simulations. We show that alloys that decompose at a macroscopic scale at equilibrium can be stabilized into three additional steady states: homogeneous and disordered, homogeneous and ordered, or ordered and decomposed in mesoscopic patterns. Consequences for the synthesis of nanocomposites by energetic ion beams are discussed.

DOI: 10.1103/PhysRevB.66.020303 PACS number(s): 64.60.Cn, 47.54.+r, 61.80.Az, 05.70.Ln

Materials in service or during their processing are often forced to exchange energy or matter with their environment. These forced exchanges, which can be seen as due to an externally imposed dynamics, drive materials into nonequilibrium configurations, stabilize new microstructures, and thus alter the material properties.[1,2] A generic approach to study these dissipative systems is provided by Ising-type models with competing dynamics:[3–6] an external dynamics drives the system away from equilibrium, while its internal dynamics tries to restore the equilibrium state. Such models have been used, for instance, to study ionic conductors driven by an external electrical field,[3] and alloys subjected to sustained irradiation[7,8,2,9] or sustained plastic deformation.[10] The control parameters of the external dynamics, hereafter referred to as the forcing parameters, determine the evolution of the system and the steady state it may reach. A crucial question therefore resides in the proper identification of these forcing parameters.

Until recently it was not clearly recognized that the characteristic length of the external dynamics is an important forcing parameter. This point may be fully appreciated by considering the case of alloys under irradiation. Indeed, the forced atomic relocations induced by nuclear collisions are distributed around a characteristic length R. This length can be varied from one nearest-neighbor distance to a few nanometers by varying the irradiation conditions.[11] If the alloy can be fully characterized by its composition, which is a globally conserved order parameter, it has been predicted[12,13] that the material can spontaneously self-organize into nanoscale compositional patterns when R exceeds a critical value R_c. Recent experimental observations of irradiation-induced compositional patterns are consistent with this prediction.[14,15]

In many situations, however, the proper description of a system requires more than one order parameter, which could be nonconserved, e.g., the degree of chemical order.[16,2] Prior studies on driven systems with coupled conserved and nonconserved order parameters[17–19] have not investigated the role of the relocation range R, with the exception of one study[20] that suggests that self-organization may take place, based on the wave-vector dependence of a mean-field nonequilibrium free energy.

We address here this question by studying a generic A_cB_{1-c} alloy system driven by random jumps with a finite range R. Borrowing from the case of alloys under irradiation, we refer to this dynamics as the ballistic dynamics.[7] At thermodynamic equilibrium, this alloy decomposes at a macroscopic scale into an A-rich ordered phase and an A-lean disordered solid solution. When the alloy is driven away from equilibrium, we show that three new steady states can be stabilized, including a self-organized state. The conditions for stabilizing this patterned state, however, become more stringent as the driving force for chemical ordering increases.

We consider an A_cB_{1-c} binary alloy on a face-centered-cubic (fcc) lattice. There are pairwise atomic interactions between first and second nearest neighbors, V_i^{XY} with $X,Y=A,B$ and $i=1,2$. Defining ordering energies as $V_i=V_i^{AB}-V_i^{AA}/2-V_i^{BB}/2$ for $i=1, 2$, we choose $V_1=-0.08$ eV and $a=-V_2/V_1=2/5$ so as to stabilize at equilibrium a phase coexistence between an A-lean fcc solid solution ($A1$ phase) and an A-rich $L1_2$ ordered phase. In the absence of dynamical forcing, Abinandanan *et al.*[21] used kinetic Monte Carlo (KMC) simulations to analyze the ordering and decomposition reactions that take place during annealing in this alloy system. In this work the temperature is fixed at $T=0.09$ eV, and we restrict ourselves to nominal compositions inside the $A1$-$L1_2$ two-phase field, i.e., $0.06<\bar{c}<0.21$ in the mean-field model and $0.10<\bar{c}<0.20$ in the MC simulations.

We first study this model alloy using a continuum one-dimensional mean-field model, with the local composition c and the local degree of order S as conserved and nonconserved order parameters. For a self-consistent derivation,[22] we start with a microscopic description. We consider a stacking of {111} planes: each plane is then equivalent with respect to the $A1$ and $L1_2$ phases, and it can be decomposed into sites on an α sublattice (of proportion 1/4) and a β sublattice (of proportion 3/4). In the $L1_2$ phase, B atoms occupy preferentially the β sites. The local composition and degree of order are related to sublattice occupation probabilities for A atoms on a given plane through: $c=(C_\alpha^A+3C_\beta^A)/4$ and $S=(C_\alpha^A-C_\beta^A)/(4c)$. Simple algebra yields the

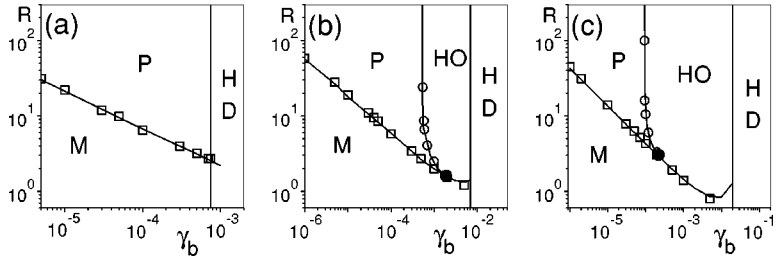

FIG. 1. Predicted dynamical phase diagrams based on instabilities obtained from analytical (lines) and numerical (symbols) stability analyses of the continuum model: (a) $\bar{c}=0.10$, (b) $\bar{c}=0.12$, and (c) $\bar{c}=0.15$. R is the characteristic range of the forced atomic relocations in units of the (111) interplanar spacing d_{111}. γ_b is a reduced forcing frequency (see text for definition). Four domains are identified: homogeneous and disordered (HD), homogeneous and ordered (HO), ordered and decomposed at a macroscopic scale (M), and ordered and decomposed into mesoscopic patterns (P).

total free energy of a given $[c(x),S(x)]$ profile as a discrete sum over the plane index, and its continuum counterpart is

$$F[c,S]=\int dx\left[f(c,S)+\frac{1}{2}N_c(\nabla c)^2+\frac{1}{2}N_s(\nabla S)^2\right]$$

with

$$f(c,S)=Z_0V_1c^2\left[-\left(1-\frac{a}{2}\right)+S^2\left(1+\frac{3a}{2}\right)\right]+\frac{kT}{4}[P(c+3cS)+3P(c-cS)]. \quad (1)$$

where $N_c=2zV_1[1-a-S^2(1+3a)]$, $N_s=-2zV_1c^2(1+3a)$, Z_0 and z are the total and interplane coordination numbers ($Z_0=12$, $z=3$), and $P(x)=x\ln(x)+(1-x)\ln(1-x)$. Note that N_c and N_s are function of c and S, contrary to assumptions sometimes made.[23]

We now turn to a kinetic description of this model alloy in the presence of competing dynamics. For the thermal dynamics we use the classical expressions for an alloy with conserved and nonconserved order parameters, the so-called "model C."[16] For the forced dynamics, we derive from the above microscopic model the rates of variation of c and S as a function of R and Γ_b, the ballistic jump frequency. The probability distribution of ballistic relocation distances, w_R, is chosen to be a decaying exponential with a decay length R. Indeed this functional dependence fits well molecular-dynamics simulation results of displacement cascades in irradiated solids.[24] It also enables us to perform analytic calculations. The resulting kinetic equations are:

$$\frac{\partial c}{\partial t}=M_c\nabla^2\frac{\delta F}{\delta c}-\Gamma_b(c-\langle c\rangle_R), \quad (2)$$

$$\frac{\partial S}{\partial t}=-M_s\frac{\delta F}{\delta S}-\Gamma_bS, \quad (3)$$

where $\langle c\rangle_R$ is the local composition convoluted by w_R.[12] The ballistic terms are simplified expressions that are strictly valid when R is large. The thermal mobility coefficients M_c and M_s are calculated in a self-consistent manner.[19] In order to obtain analytical results, another simplification is made: these mobilities are evaluated for a homogeneous disordered state. This yields $M=M_c/M_s=(9\bar{c}^2d_{111}^2)/16$.

We can study the local stability of steady states in this driven alloy by performing a linear stability analysis. For small perturbations of the form $\exp(\omega t+ikx)$ around a homogeneous steady-state profile $(\bar{c},\bar{S})$, the perturbation amplitudes $(\delta c,\delta S)$ are solution of[23]

$$\begin{bmatrix}A_{11} & A_{12}\\ A_{21} & A_{22}\end{bmatrix}\begin{bmatrix}\delta c\\ \delta S\end{bmatrix}=-\omega\begin{bmatrix}\delta c\\ \delta S\end{bmatrix} \quad (4)$$

with $A_{22}=M_s(f_{ss}+k^2N_s)+\Gamma_b$,

$$A_{11}=M_ck^2(f_{cc}+k^2N_c)+\Gamma_bR^2k^2/(1+R^2k^2),$$

$$A_{12}=M_ck^2f_{sc},\quad A_{21}=M_sf_{sc}, \quad (5)$$

where we used the notation $f_c=(\partial/\partial c)f$, etc. The two dispersion branches are given by ω_1 and ω_2, the eigenvalues of $(-A)$. Instabilities will take place when one or both eigenvalues become positive in some wave-vector interval.

Let us first consider the evolution of an alloy initially disordered and homogeneous, e.g., obtained by quenching from a high-temperature state. We restrict our analysis to compositions larger than the ordering spinodal composition ($c_{os}=0.0975$ at 0.09 eV): the initial state is then stable with respect to composition fluctuations but unstable toward continuous ordering,[25] provided that $\Gamma_b<\Gamma_{b,(1)}=-M_sf_{ss}$ (note that f_{ss} is negative for $c>c_{os}$). In this case, inspection of Eqs. (2) and (3) reveals that there exists another homogeneous steady-state solution, which has a nonzero degree of order. This steady state thus corresponds to a long-range ordered state.

We now perform a second linear stability analysis to determine the domain of stability of this ordered state. For that purpose, we recalculate the dispersion equations because the coefficients in Eq. (5) depend on the degree of order. In the absence of ballistic jumps, and for the compositions discussed below (see Fig. 1), this second steady state is unstable with respect to spinodal decomposition.[25] In the presence of the ballistic dynamics, however, two additional situations are found: the homogeneous ordered state may be locally stable, or it may become unstable toward decomposition, but only

for an interval of wave vectors that has a nonzero lower bound. By extension of our work on alloys with one conserved order parameter with ballistic jumps,[12] we anticipate that this last reaction will lead to self-organized patterns. Four stable steady states are therefore predicted to be possible: a homogeneous disordered (HD) state, a homogeneous ordered (HO) state, a state decomposed at the macroscopic scale (M), and a state decomposed at a mesoscopic scale (P), i.e., with patterns. Note that the homogeneous ordered steady state can also be stablized by short-range ballistic jumps.[18]

The boundary for the HO→M instability can be obtained analytically since it corresponds to the (R, Γ_b) values for which the curvature of the eigenvalue responsible for spinodal decomposition changes its sign at $k=0$. Defining a reduced ballistic frequency by $\gamma_b=\Gamma_b/M_s$, this second boundary is given by

$$R_{(2)}^2=\left[\frac{f_{sc}^2}{f_{ss}-\gamma_b}-f_{cc}\right]\frac{M}{\gamma_b} \quad \text{for} \quad \gamma_b<\gamma_{b,(1)}. \tag{6}$$

The determination of the HO→P instability is more delicate since it takes place at a nonzero and nonconstant wave vector. By inspection of the leading terms, we derive an approximate expression for this third boundary:

$$R_{(3)}^2=\left[\frac{Q}{(\gamma_b-\gamma_b^c)}\right]M \quad \text{for} \quad \gamma_b^c<\gamma_b<\gamma_{b,(1)}, \tag{7}$$

with $\gamma_b^c=Q^2/N_c$, and $Q=(f_{sc}^2-f_{cc}f_{ss})/2f_{ss}$. These three instability boundaries are plotted in Fig. 1 for three nominal compositions, $\bar{c}=0.10$, 0.12, 0.15, in the (R,γ_b) plane. In all cases the boundaries determined analytically are in excellent agreement with full numerical solutions. It is predicted that the $\bar{c}=0.10$ alloy can reach three different steady states, HD, M, and P, similar to our previous results on alloys with one conserved order parameter.[12] As $\bar{c}$ increases, however, a new field (HO) appears, where the homogeneous ordered state remains (locally) stable. Furthermore, the boundaries HO →M and HO→P intersect at $R=R_c$, and for R values lower than R_c only the HO→M instability remains [boundary (2)]. As $\bar{c}$ is increased to 0.15, the HO field becomes wider and the minimum relocation distance necessary to stabilize patterns, R_c, becomes larger.

The above kinetic mean-field model suffers from several limitations. In particular, the calculated phase boundaries relate to local stability, whereas we are interested in the global stability of these steady states, and the alloy may reach steady states other than those considered so far. To overcome these limitations, we performed KMC simulations on a three-dimensional fcc lattice with the same pairwise interactions used previously (see Ref. 13 for details). Crystals with L^3 sites, $L=32$, 64, 128, are used with a fixed vacancy concentration c_v. Atoms migrate either by exchanging their site with a first nearest-neighbor vacancy, through a thermally activated process, or by atom-atom permutations at a ballistic frequency Γ_b weighted by the relocation distance probability w_R.

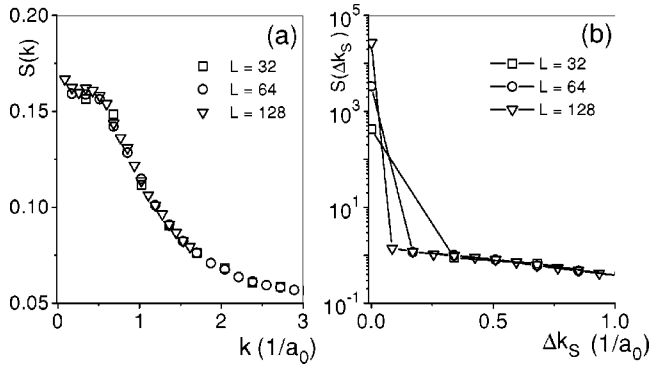

FIG. 2. KMC structure factors at steady state, spherically averaged (a) near the Bragg peak and (b) near the superlattice reflection ($\Delta k_s=|\mathbf{k}-\mathbf{k}_s|$). With forcing parameters $R=\sqrt{54}$ and $\Gamma_b/c_v=2.6\times10^5$ s^{-1}, corresponding to $\gamma_b=4\times10^{-4}$, this $\bar{c}=0.15$ alloy is stabilized into a homogeneous long-ranged ordered state (HO), as assessed by the crystal size (L) dependences of $S(k)$ and $S(\Delta k_s)$.

The steady states are determined by analyzing structure factors centered around $\mathbf{k}=0$, the Bragg peak, and around $\mathbf{k}_s=\{100\}$, the $L1_2$ superlattice reflections. These structure factors are first calculated along the trajectory of the system, then spherically averaged, and then time averaged to ensure that steady state has been reached.

The characteristics of these averaged structure factors clearly identify the steady states: disordered or short-range ordered states present near $\mathbf{k}_s$ small intensities that are independent of the crystal size; long-range ordered states, on the contrary, give rise to large intensities that scale with the simulation volume [see Figs. 2(b) and 3(b)]. Phase decomposition is similarly assessed by analyzing the structure factors near $\mathbf{k}=0$: mesoscopic states are identified by the presence of a crystal size independent peak for a nonzero wave vector near $\mathbf{k}=0$ [Fig. 3(a)], whereas macroscopic decomposition is identified by a Bragg peak whose intensity scales with the simulation volume.

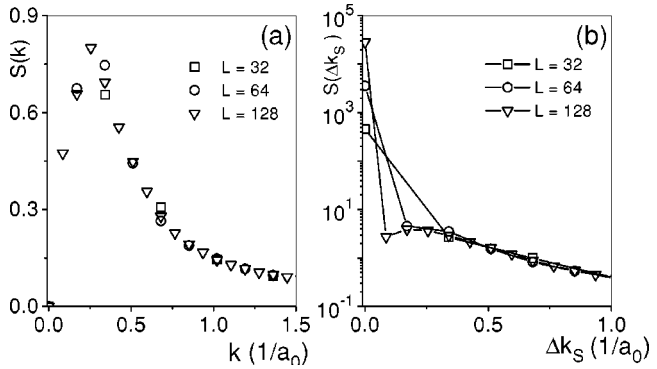

FIG. 3. KMC structure factors at steady state, spherically averaged (a) near the Bragg peak and (b) near the superlattice reflection ($\Delta k_s=|\mathbf{k}-\mathbf{k}_s|$). With forcing parameters $R=\sqrt{54}$ and $\Gamma_b/c_v=2.6\times10^4$ s^{-1}, corresponding to $\gamma_b=4\times10^{-5}$, this $\bar{c}=0.15$ alloy is stabilized into a state decomposed at a finite scale between long-range ordered and disordered regions (P), as assessed by the crystal size (L) dependences of $S(k)$ and $S(\Delta k_s)$.

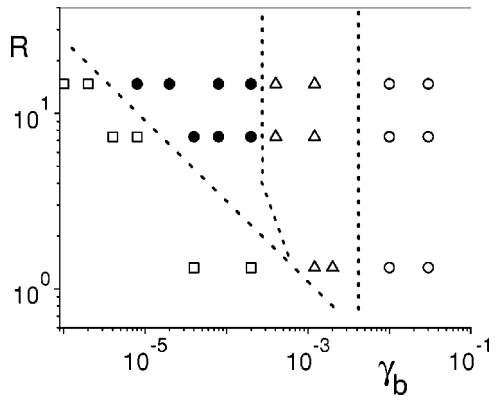

FIG. 4. KMC (R, γ_b) dynamical phase diagram for $\bar{c}=0.15$. The symbols correspond to following states: M (□), P(●), HO (△), and HD (○). The dashed lines are approximate locations of the phase boundaries.

The KMC results obtained for $\bar{c}=0.15$ are summarized in Fig. 4. The four steady states identified by linear stability analysis, and only those, are observed. The topology of the KMC phase diagram is in very good agreement with the analytical calculations [see Fig. 1(c)]. For comparison with the analytical model, the average thermal vacancy jump frequency is measured during thermal equilibrium KMC simulations, and is used to rescale the ballistic jump frequency to obtain a reduced ballistic frequency γ_b. For $\bar{c}=0.12$ (not shown here), the homogeneous ordered field is greatly reduced, in agreement with the analytical predictions.

The present work points to the rich phenomenology that results from the coupling between ordering and decomposition in alloys driven by forced mixing with finite range. From a practical viewpoint, the competition between patterning and homogeneous ordering has an important consequence: the minimum relocation range R_c required to stabilize patterns increases with $\bar{c}$. For dilute alloys this minimum range is small enough so that the actual range during ion-beam processing may exceed R_c. Thus we predict that patterning can take place under appropriate irradiation conditions, and indeed it has been recently observed in Ni-irradiated Ni-12%Al.[19] For more concentrated alloys, however, as the maximum relocation range produced by ion irradiations is $\sim 1-2$ nm,[11] patterning should no longer be possible.

We thank R. S. Averback, D. Cahill, R. A. Enrique, and S. Granick for stimulating discussions. This material is based upon work supported by the US Department of Energy, Basic Energy Sciences, Grant No. DEFG02-91ER45439, through the Frederick Seitz Materials Research Laboratory at the University of Illinois at Urbana-Champaign.

[1] For instance, see H. Haken, *Synergetics: An Introduction* (Springer, Berlin, 1978).
[2] G. Martin and P. Bellon, Solid State Phys. **50**, 189 (1997).
[3] S. Katz, J.L. Lebowitz, and H. Spohn, Phys. Rev. B **28**, 1655 (1983).
[4] A. De Masi, P.A. Ferrari, and J.L. Lebowitz, Phys. Rev. Lett. **55**, 1947 (1985).
[5] P.L. Garrido and J. Marro, Phys. Rev. Lett. **62**, 1929 (1989).
[6] B. Schmittman and R.K.P. Zia, in *Phase Transitions and Critical Phenomena*, edited by C. Domb and J.L. Lebowitz (Academic Press, London, 1998), Vol. 17, and references therein.
[7] G. Martin, Phys. Rev. B **30**, 1424 (1984).
[8] V.G. Vaks and V.V. Kamyshenko, Phys. Lett. A **177**, 269 (1993).
[9] R.A. Enrique and P. Bellon, Phys. Rev. B **60**, 14 649 (1999).
[10] P. Bellon and R.S. Averback, Phys. Rev. Lett. **74**, 1819 (1995).
[11] R.S. Averback and T. Diaz de la Rubia, Solid State Phys. **51**, 281 (1998).
[12] R.A. Enrique and P. Bellon, Phys. Rev. Lett. **84**, 2885 (2000).
[13] R.A. Enrique and P. Bellon, Phys. Rev. B **63**, 134111 (2001).
[14] R.A. Enrique and P. Bellon, Appl. Phys. Lett. **78**, 4178 (2001).
[15] G.C. Rizza, M. Strobel, K.H. Heinig, and H. Bernas, Nucl. Instrum. Methods Phys. Res. B **178**, 78 (2001).
[16] P.C. Hohenberg and B.I. Halperin, Rev. Mod. Phys. **49**, 435 (1977).
[17] F. Soisson, P. Bellon, G. Martin, Phys. Rev. B **46**, 11 332 (1992).
[18] S. Matsumura, S. Muller, and C. Abromeit, Phys. Rev. B **54**, 6184 (1996).
[19] G. Schmitz, J.C. Ewert, F. Harbsmeier, M. Uhrmacher, and F. Haider, Phys. Rev. B **63**, 224113 (2001).
[20] V.G. Vaks and S.V. Beiden, Phys. Lett. A **182**, 140 (1993).
[21] T. Abinandanan, F. Haider, and G. Martin, Acta Mater. **46**, 4243 (1998).
[22] G. Martin, Phys. Rev. B **41**, 2279 (1990).
[23] H.P. Fischer and W. Dieterich, Phys. Rev. E **56**, 6909 (1997).
[24] R.A. Enrique, K. Nordlund, R.S. Averback, and P. Bellon (unpublished).
[25] S.M. Allen and J.W. Cahn, Acta Metall. **24**, 425 (1976).